Monohull ship hydrodynamic simulation using CFD

Paúl Sebastián Dávila Aldás,
Jessica Constante and
Gabriela Chávez Tapia

Instituto Nacional de Eficiencia Energética y
Energías Renovables – INER,
Quito, Ecuador
Email: paulgat9@hotmail.com
Email: jessica.constante@iner.gob.ec
Email: gabriela.chavez@iner.gob.ec

Javier Martínez-Gómez*

Instituto Nacional de Eficiencia Energética y
Energías Renovables – INER,
Quito, Ecuador
and
Universidad Internacional SEK Ecuador,
Quito, EC170134, Ecuador
Email: javiermtnezg@gmail.com
*Corresponding author

Abstract: This research analyses the performance of a ship monohull at Galapagos real conditions using ANSYS FLUENT. In order to achieve these analyses, tide charts at Santa Cruz Island coast in Galapagos Islands were considered, since similar motorboats provide services as taxi boats in this area. These analyses were made in order to validate ships behaviour existing in Galapagos Islands. In addition, through simulation is not necessary to build these ships, in a way to obtain same results using less economic and technical resources. The hydrodynamic analysis of a monohull was simulated in static and dynamic conditions. Static analysis considers water and air flows hitting the boat bow which is resting (anchored boat). While dynamic analysis considers both the boat and water flow speed (sailing boat). Main results were: static and dynamic pressures, water height achieved by flow and ship speed variation, turbulence intensity, and simulation convergence residuals.

Keywords: monohull; hydrodynamics simulation; ANSYS-FLUENT; computational fluid dynamics; CFD.

Reference to this paper should be made as follows: Aldas, P.S.D., Constante, J. and Tapia, G.C. and Martínez-Gómez, J. (2019) 'Monohull ship hydrodynamic simulation using CFD', *Int. J. Mathematics in Operational Research*, Vol. 15, No. 4, pp.417–433.

Biographical notes: Paúl Sebastián Dávila received his Mechanical Engineering degree from the Escuela Politécnica del Ejército in 2012; Master's in Design, Production and Automation of the National Polytechnic School in the city of Quito in 2015. Currently, he works as a Technical Analyst at the

National Institute of Energy Efficiency and Renewable Energy, in addition to providing services as a teacher at the School. National Polytechnic His thesis is related to the design of machines and aeromodelling, professional experience in oil services, modelling and simulation of machines and mechanical systems, metal structures and quality management systems.

Jessica Constante received her degree in Electronic Engineering, Robotics and Mechatronics in 2014 from the Equinoctial Technological University. She is currently a Technical Analyst of the National Institute of Energy Efficiency and Renewable Energy since May 2013.

Gabriela Chávez Tapia received her degree in Electronic Engineering, Robotics and Mechatronics in 2016 from the Equinoctial Technological University. She is currently a Technical Analyst of the National Institute of Energy Efficiency and Renewable Energy since May 2016.

Javier Martínez-Gómez received his Industrial Engineering degree from the Carlos III University at Madrid in 2008 and Master's in Materials Science and Engineering at the Universidad Carlos III de Madrid in 2010. He received his PhD in Materials Engineering Science from the Universidad Carlos III de Madrid in 2013. His fields of research are related to clean cooking, multicriteria decision methods and material science. He currently works as a Postdoctoral Researcher at the National Renewable Energy Institute, INER and as a Lecturer at the Universidad Internacional SEK (UISEK).

1 Introduction

Generally, to perform an analysis and design of an engineering application, the solution bifurcates into construction of a prototype and simulation (Martínez-Gómez, 2018; Villacreses et al., 2017; Godoy-Vaca et al., 2017). Prototype construction has as principal inconveniences cost and scaling results in real conditions (Acharya and Biswal, 2016; Villacís et al., 2015; Beltran et al., 2017). While modelling through simulation in software leads to obtain the same results, yet spending less technical and economic resources (Azimi and Solimanpur, 2016; Chaloob et al., 2016; Heidarzade et al., 2016). Simulation examples can be found at Anderson and Coughlan (2006) study liquid film flows over solid surfaces. Boutchel et al. (2004) performed studies using wind tunnels to optimise real rime rain situations. Furthermore, Gaylard and Duncan (2011) studied the rear glass and body side vehicle soiling by road sprays. Roettger et al. (2011) studied contamination effects through adhesion of solid particles. In addition, Wu and Cui (2009) performed an investigation in pools using a scale cargo ship, to see its behaviour through swell.

The fast develop of computational and numeric methods, as computational fluid dynamics (CFD), have come side by side with the advance of computers (Kastillo et al., 2015, 2017). CFD focuses on wide diffusion modelling that uses numeric methods and simulations on a computer to solve and analyse problems that involve flow transportation phenomenon (Montiel et al., 2013). Fluid dynamics investigation examples applied to means transport using CFD have been performed, for example Damjanović et al. (2010), accomplished an aerodynamic modelling of a car using Fluent, in which a 2D analysis of the side contour of the car was achieved. Hagemeier et al. (2011) analyse the expulsion of

gases generated by an urban vehicle. The results of this research were analysed by OpenFOAM CFD software and validated by wind tunnel tests.

There is a limited number of information referring to navy analysis and design applied to monohulls with fluid dynamics. In the same way examples can be found at Hirdaris et al. (2014) evaluated structural responses in ship designs, offshore, in which the results are validated by lineal and non-lineal mathematic models. Yarrarapu et al. (2015) analysed the importance of a stabiliser to determinate the ship route using CFD in ANSYS FLUENT. Likewise, Kulczyk and Gornicz (2014) performed the analysis of motorboats in which a comparative study of dynamic adjustment and free surface resistance were accomplished using ANSYS FLUENT and fine/marine.

Therefore, many sub models stay heuristic and do not represent an efficient design base for different ship models. For that reason, it is of special interest to work with a software that can get as close as possible to operating conditions as K–ω SST model of ANSYS FLUENT. The simulating model standard k-w, relates kinetic energy 'k' of the system and the frequency of a turbulent flow 'ω'. This model predicts transition that is generated from flow at the ship walls. This model uses the hypothesis of gradient velocity diffusion by relating Reynolds number and turbulent viscosity. Its principal advantage comes from the mesh identification of the frontier layer of the boat in order to perform a detailed analysis and handle a complex limit layer under pressure gradient. As principal disadvantage the resolution of the mesh closer to the ship walls in contact with water and air flows requires to be manually entered until it reaches convergence (Dash et al., 2015) K–ε model solver of ANSYS FLUENT is not accurate with flows that exhibit strong curvature, and K–ω is more useful in this case. Through the development of the simulation, K–ε model did not converge and created massive flaws with water/air flows. Studies about this matter were performed by Singh et al. (2014) to design sport utility vehicles as a result of friction reduction. Furthermore, Yarrarapu et al. (2015) studied the influence of a stabiliser at stern to analyse the stability of a ship hull.

This research tries to expand the information of navy analysis applied to monohulls with fluid dynamics. This study analyses the behaviour of a ship monohull at Galapagos Islands by K–ω SST model of ANSYS FLUENT. These conditions were taken from the Army oceanographic institute of Ecuador (INOCAR) that has tide charts which are annual publications of tide predictions and measurements in 20 ports along the coast of Ecuador and Galapagos (INOCAR, 2015). These current and tidal charts at Santa Cruz Island coast in Galapagos Islands were taken as parameters, because of the use of similar motorboats that work at the coast. Critic sailing conditions were studied, in a way to analyse and correct the advance of the ship monohull, its structure and geometry as well, because they are related to the strains the ship bears and its minimum resistance of unit area that the ship material must have. The simulation considers wind and tidal velocity parameters for the anchored case (static) and offshore (dynamic). The results are validated by theoretical values of static and dynamic pressures. The contribution of this investigation is to study passengers and cargo transportation existing at Galapagos Islands, as an informative base for further and future ship construction making a previous efficient design in order to avoid a rush purchase of a ship. Using ANSYS FLUENT to analyse strains, and ship geometry without having to build the ship.

The rest of the research is organised as follows: The suggested methodology is described in Section 2. The data results and discussion are presented in Section 3. The most important conclusion or the work is detailed in Section 4.

2 Fundamental relations

The simulation pretends to emulate real working conditions of the monohull to analyse hydrodynamic characteristics and turbulence in operating conditions. The simulation has been performed using CFD with finite volume method (FVM) since ANSYS FLUENT makes the analysis using this method FVM. Solidworks has also been applied to design the model. The geometry of the model, as a problem discretisation, its solution and subsequent-process were carried out in software ANSYS FLUET v16.0. Using a computer with i7 processor, 4 GB RAM memory and 750 GB of internal storage.

To perform a FVM simulation, it is necessary to do a sequence of steps, in which are defined and restricted simulating conditions. Consequently, activities are described as following, considering sequence and analysis parameters for each case.

The rest of the material and methods is organised as follows: The geometry projection and experimental equipment are described in Section 2.1. The physical model is presented in Section 2.2. The general simulation parameters are detailed in Section 2.3. The FVM of discretisation is presented in Section 2.4. In Section 2.5, the mesh is described in. Finally, the results of the validation process are detailed in Section 2.6.

2.1 Geometry projection and experimental equipment

The geometry of the ship has to prove that it is safe facing shore swell and through offshore journey. Propulsion must guarantee the operation speed of at least seven knots (13 km/h). The geometry of the monohull was projected with the dimensions of a boat type (Segura and Remigio, 2016). For principal dimensions see in Table 1:

Table 1 Simulated ship dimensions

Description	*Units*	*Dimension*
Total length	Metres	7.5
Beam	Metres	1.8
Prop	Metres	0.9
Gross register tonnage (GRT)	Tonnage	2.59
Net register tonnage (NRT)	Tonnage	0.78

Principal shapes of the monohull were modelled, considering navy criteria such us lift force, buoyancy and stability. In addition, geometry and profile ships that work at the coast of Ecuador was consider (Bartrons-Casademont, 2014; Shao and Faltinsen, 2012).

This model was performed using modelling 3D tools as Solidworks and compatibility with ANSYS FLUENT software.

2.2 Physical model

Equations for fluid dynamics are based on momentum transport and continuity equations. Fluent uses FVM that implies discretisation and integration of the governing equation of volume control (Jongebloed, 2008).

Turbulent kinetic energy, k, and the specific dissipation rate, ω, are obtained from transport equations (1) and (2) (ANSYS, 2009):

$$\frac{d}{dt}(\rho k)+\frac{d}{dx_i}(\rho k u_i)=\frac{d}{dx_i}\left(\Gamma_k \frac{dk}{dx_j}\right)+G_k-Y_k+S_k \tag{1}$$

$$\frac{d}{dt}(\rho \omega)+\frac{d}{dx_i}(\rho \omega u_i)=\frac{d}{dx_i}\left(\Gamma_\omega \frac{d\omega}{dx_j}\right)+G_\omega-Y_\omega+S_\omega \tag{2}$$

where ρ is fluid's density; G_k and G_ω represent the turbulent kinetic energy generated by velocity gradients in different sections of the ship analysis; Γ_k and Γ_ω represent diffusive effective of k and ω; Y_k and Y_ω represent k and ω dissipation due to turbulence; S_k y S_ω are defined terms by ANSYS FLUENT for each analysis model and they refer to defined mesh and vorticity magnitude.

Effective diffusivity for k and ω model, which its value defines turbulence intensity generation, is given by the equations (3) and (4):

$$\Gamma_k=\mu+\frac{\mu_t}{\sigma_k} \tag{3}$$

$$\Gamma_\omega=\mu+\frac{\mu_t}{\sigma_\omega} \tag{4}$$

where σ_k and σ_ω, are turbulent Prandtl numbers for k and ω. Turbulent viscosity, μ_t, comes from the combination of k and ω as shown in equation (5):

$$\mu_t=\alpha^*\frac{\rho k}{\omega} \tag{5}$$

The α^* coefficient smooth turbulent viscosity, accepting a corrective low Reynolds number. It is defined by equation (6):

$$\alpha^*=\alpha^*_\infty\left(\frac{\alpha^*_0+\frac{K_{\varepsilon_t}}{K_k}}{1+\frac{R_{\varepsilon_t}}{R_k}}\right) \tag{6}$$

where:

$$R_{\varepsilon_t}=\frac{\rho k}{\mu\omega} \tag{7}$$

$$R_k=6 \tag{8}$$

$$\alpha^*_0=\frac{\beta_i}{3} \tag{9}$$

$$\beta_i=0.072 \tag{10}$$

It must be emphasised that in turbulent flow for model $k-\omega$: $\alpha^*=\alpha^*_\infty=1$.

2.3 General simulation parameters

To simplify the problem, some assumptions have been performed in order to establish initial conditions for the simulation as gravity 9.8 m/s^2, multiphasic model, implicit, open channel and disperse for the analysis model. The selection of flow type was selected as turbulent and laminar according to Reynolds. Air density was 1,225 Kg/m^3, viscosity was 1.78 e-5 Kg/ms, thermic conductivity was 0.0242 W/K and specific heat was 1,006.43 J/Kg.K. For water conditions, the following characteristics were entered: water density was 998.2 Kg/m^3; water viscosity was 0.001003 Kg/ms, thermic conductivity was 0.6 W/K, specific heat 4,182 J/Kg.K. and water temperature: 15°C, since it is the normal temperature as reference for water simulations. The application point of atmospheric pressure: was selected as reference the monohull stern, using Z axis; with the following values: coord. X: 0; coord. Y: 4; coord. Z: 2, Value: 101,325 Pa.

2.4 General simulation parameters FVM discretisation

In order to discretise the problem, the environment in which the ship will be moving, is established (open channel flow conditions) (Shao and Faltinsen, 2012), through a parallelepiped, which comprises an air mass and a water mass, same ones that offer resistance to movement.

Figure 1 Geometry sections and boundaries (see online version for colours)

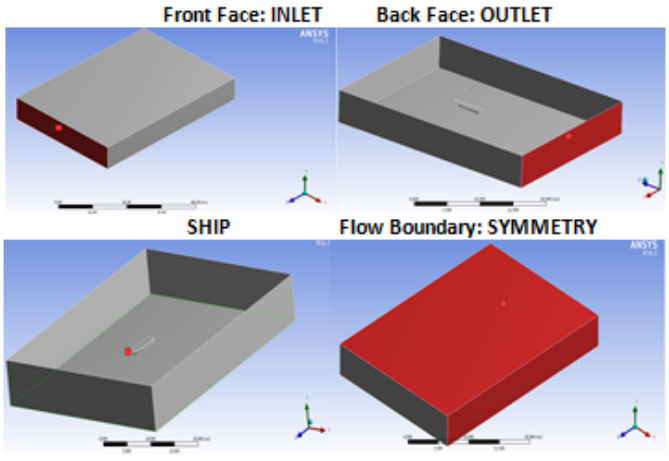

The created parallelepiped defines depth, length and width of the volume analysis and ship simulation. To the parallelepiped simplified equations (11)–(17) were applied (Shao and Faltinsen, 2012).

$$P_{Wd} = 0.5 * Sl \tag{11}$$

$$P_{Afl} => 0.5 * Sl \tag{12}$$

where 'P_{Wd}' and 'P_{Af}' are water depth and over the floating line is air. 'Sl' is the value of the ship length at the floating line.

$$A_1 = 2.5 * Sl \tag{13}$$

$$A_2 = 2.5 * Sl \tag{14}$$

where 'A_1' and 'A_2' are the cube width related to the floating line sides.

In addition, parallelepiped lengths are given by the equations (15)–(16):

$$L_1 = 3.75 * Sl \tag{15}$$

$$L_2 = 3.75 * Sl \tag{16}$$

where 'L_1' and 'L_2' are the cube length in relation to the ship plane.

Moreover, mesh operation is used to divide the solid model in smaller geometric elements, which are united by nodes (De Leval et al., 1996). In order to achieve it, the geometry formed between the ship and the parallelepiped is divided in four sections: top, bottom, and side faces of the parallelepiped. These sections establish inlet and outlet flow parameters as contours of itself.

In addition, two simulating conditions have been determinate; the first case simulates the ship resting and the current hitting it from the front side and the second case simulates the ship in movement, meaning that the ship and current have velocity. These two criteria have been defined as static and dynamic analysis.

Furthermore, both cases keep boundary conditions, and what actually varies is the ship velocity. In the static case, ship velocity is zero and the current has a constant velocity of seven knots. In the second case current has constant velocity of seven knots and the ship simulates opposite direction from 4 to 8 knots.

The boundary conditions for static and dynamic cases are the following:

As said before, swell charts and wave heights are introduced as parameters. Considering that similar boats work at Galapagos Islands. The following average was 1.0272 m. The data was obtained for two days of every week for three months (INOCAR, 2015).

Boundary conditions to solve the problem are the following: open channel flow for Sub-model of analysis; meaning that the simulation emulates a duct, in which water flows with a free surface as an open sea case. Turbulent flow type has been selected due to Reynolds values greater than 10,000. The Z axis was selected as reference frame for movement. Relative speed was selected for resistance mode; this parameter considers reversing directions of the current and the ship. The ship was selected as wall type with mobile condition; this parameter emulates the movement of the ship. The type of Analysis translational emulates the movement of the ship. In addition, it was also selected shear strain without displacement; in which this type of strain is analysed in each mesh node. The relation between intensity and viscosity was specified as analysis method; this parameter refers to the simulation, and how to analyse the relation variation of turbulence and viscosity at every point of the fluid. Finally, the minimum value was 2 mm for turbulent viscosity ratio; in which eddies are formed in zones where turbulence is generated.

Likewise, conditions for fluids (air-water) and their interactions were defined as free surface level; where it was 0 m. Wave direction was also necessary to reference as normal to boundary, which means that wave crests are generated perpendicular to forward movement of the current. It was also establishing the number of waves for the

simulation which was 2; however, it must be emphasised that swells repeat in a cyclic way and depend on the number of iterations that are defined in the simulation.

2.5 Mesh

In order to perform the mesh over the projected geometry, the model of the ship monohull must be imported to ANSYS FLUENT so that it will proceed to do the FVM process. The implementation of the mesh is done over the compound geometry of air, water and ship volume as shown in Figure 2. The used meshing tool was assembly meshing cut cell hex dominant algorithm and high smoothing (Shao and Faltinsen, 2012). Five different configurations of mesh were used, so that, the k–ω model manages to convergence.

Figure 2 Mesh obtained at the geometry contour (see online version for colours)

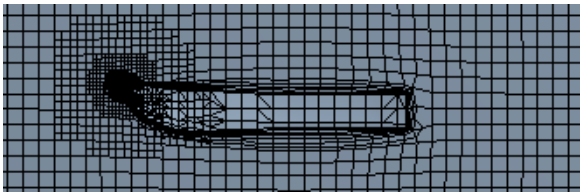

Note: Finest meshing at prow because of the complex geometry in the zone.

As it is shown in Figure 2, there was a finest size of mesh at the ship prow due to a more complex geometry at this area than the rest of the ship. Therefore, the software divides this space into smaller cells. The mesh was defined with the following characteristics in Table 2.

Table 2 Simulated ship dimensions

Attribute	*Description*
Maximum element size	0.4050 m
Minimum element size	5.06 e –0.002 m
Transition ratio	0.272 m
Cell rate of increase	1.2
Assembly method	Cutcell
Number of nodes	303,607
Number of elements	251,297

So as to solve the equations used in the mathematical model, a rectangular free mesh was built with extra-fine resolution to ensure the model convergence. The process was able to convergence in an average of 300 iterations, at 180 timesteps. The cycle was complete with approximately ten hours of non-interrupted work. Visually the ship monohull is under contact with water, until it reaches the height of the ship draft, it is not sunken and there are not water eddies formed. The results show coherence, taking into account the water height. When results went wrong, the ship monohull either was floating, completely sunken, or flow mass was out of control.

2.6 Results of the validation process

The main parameters taken into consideration for the validation process are static and dynamic pressures since they constitute fundamental variables to consider.

The obtained values from de dynamic fluid analysis by means of the simulation were verified through the use of theoretical equations: height (for static pressure) and velocity (for dynamic pressure).

Static simulation was performed through the boundary condition 'velocity inlet'. The established parameters in this boundary allow giving translational speed to both fluids that intervene in the simulation (water and air). With the objective of validating static pressure values obtained in the simulation, the process leads to find static pressure data. To accomplish it, the following equation has been used (de Paz, 2011):

$$P_{stat} = \rho_{Fluid} * g * h_{sum} \tag{17}$$

where P_{st} is calculated static pressure, $\rho_{liq.}$ is fluid density and h_{sum} is submersion height

At this point it is needed to emphasise that the ship immersion will vary with the pass of waves. In the case of static analysis, this immersion height must be staying lower than the defined draft level. In the case of this project is 0.3 m. In addition, the value must stay below de value of the ship prop 0.9 m.

Ship movement inertia produces an additional increase of the static pressure, when it hits over an area which is perpendicular to movement (ANSYS, 2015). This force is produced by the action of pressure known as dynamic. Dynamic pressure depends on the fluid velocity and density. Its calculating formula is the following:

$$P = \frac{1}{2} \rho_{fluid} * v_{fluid}^2 \tag{18}$$

where P is dynamic pressure; ρ_{fluid} is water density and v_{fluid} is water current velocity (speed).

In order to validate calculations thrown by ANSYS FLUENT simulation, it is proceeded to perform manual calculations of the static case of study. As initial value, the simulated pressure will be taken and as evidentiary result the simulation velocity.

3 Results

3.1 Static analysis

This section presents the results when the ship stays static and marine currents come forward to the ship with 4 to 8 knots of speed. The results of static and dynamic pressures, Reynolds number, turbulence intensity, water height reached, different axis strain, and convergence residuals for the static case are presented in Table 3. It shows that the values of pressure proportionally increase with the velocity, reaching as maximum value 5.96 MPa at eight knots of current speed.

The static analysis results are presented in Figure 3. The referential speed value was seven knots (3.6 m/s) of the ship, because, it is considered a real translation speed for transportation of cargo and/or passengers (Segura and Remigio, 2016). As marine current speed increases from 4 to 8 knots (2.06 a 4.12 m/s), the values of static and dynamic

pressures reach a maximum value of 1.63 and 5.96 MPa. These values are found at the hull of the ship.

Figure 3 Static analysis results, (a) static pressure, (b) dynamic pressure, (c) Reynolds number, (d) fluid turbulence, (e) water height reached in the simulation (see online version for colours)

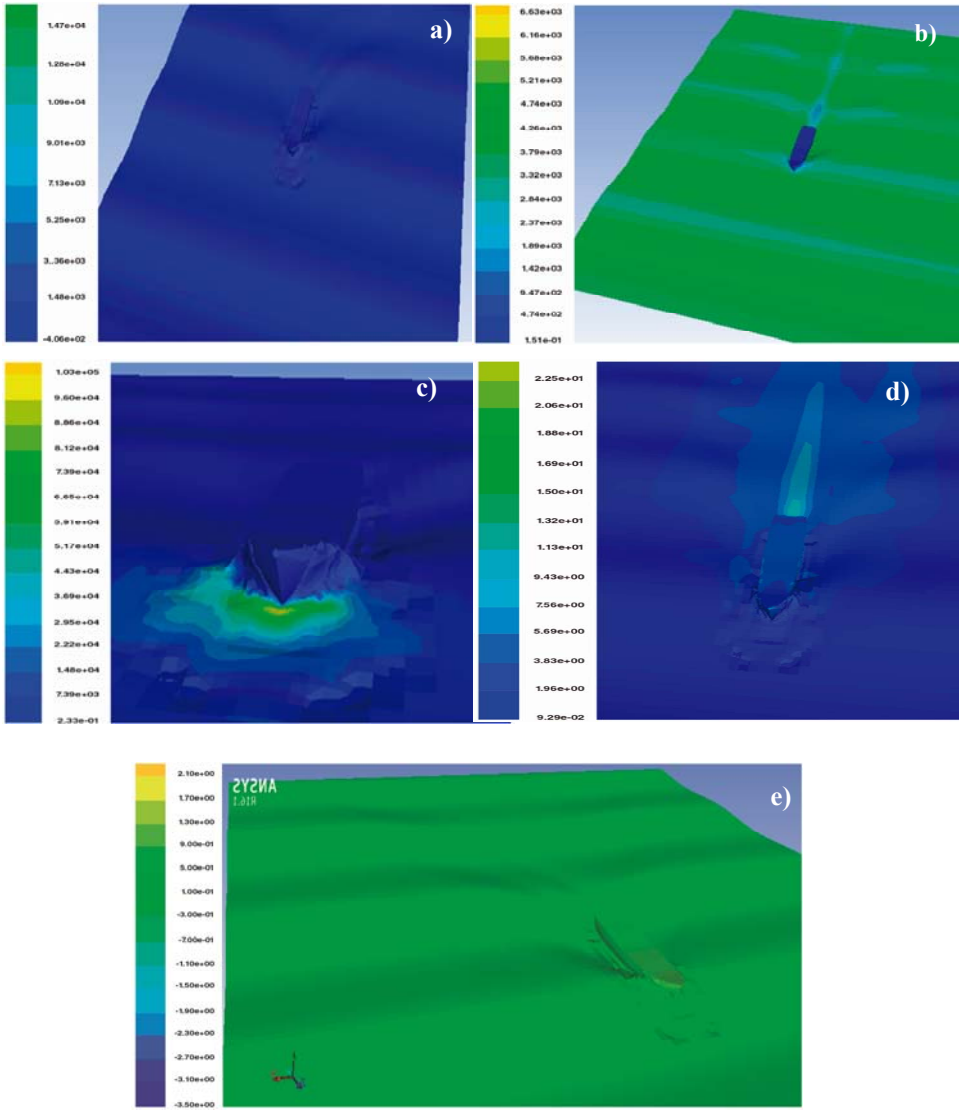

The results of Reynolds number in the contact area fluid-hull and fluid turbulence are generated as a result of the marine current movement. During the simulation, Reynolds number reaches 857.000 at the ship prow, which is the zone where major fluid turbulence is generated. Due to frontal geometry of the ship, it allows to break waves when they hit the ship. It is shown that increasing current speed and turbulence intensity decreases 42%.

Table 3 Results from the static analysis in relation to static, dynamic pressures, Reynolds number, turbulence intensity, water height reached during the simulation, different axis strains and convergence residuals

Current speed	*Static pressure [Pa]*	*Dynamic pressure [Pa]*	*Reynolds number -*	*Turbulence intensity %*	*Height [m]*	*Y strain [Pa]*	*Z strain [Pa]*	*Convergence residuals [Kg/s]*
4 knots–2.06 m/s	1,039.32	1,548.12	6.83E+05	32.3	0.10	0.19	0.049	0.001
6 knots–3.09 m/s	1,134.86	3,031.11	9.20E+05	25.7	0.12	0.14	0.056	0.0001
7 knots–36 m/s	1,515.42	4,419.08	7.53E+05	21.7	0.14	0.24	0.09	0.0002
8 knots–4.12 m/s	1,630.24	5,968.4	857,033.4	19	0.50	0.39	0.12	–0.00009

Water height from the lower end of the prow, rises when fluid speed increases to 0.5 m for eight knots. This value is reached at the bow of the ship.

3.2 Dynamic analysis

In the case of dynamic analysis, the marine currents have a speed of four knots, while the ship has a translation speed that varies from 4 to 8 knots, meaning that this simulation corresponds to the offshore ship. This reasoning explains relative speed concept, since the ship moves through water surface, is taken as constant speed.

The results from the dynamic analysis in relation to static and dynamic pressure, Reynolds number, turbulence intensity, water height reached during the simulation, different axis strains and convergence residuals are shown in Table 4.

Similar results in Figure 4 were performed for the dynamic analysis. Static and dynamic pressures increase directly proportional to ship velocity until they reach maximum values of 2.44 and 7.95 MPa. Results of maximum absolute pressure (static + dynamic) obtained from the ship reaches a value of 10.4 MPa at eight knots of speed. In addition, these values allow to define hull minimum material resistance of 0.005 N in a minimum applied area of 1 cm^2.

The zone with higher turbulence intensity can be found at the ship stern unlike the static case. At eight knots of maximum ship speed, there is a maximum turbulence value of 41.2%, 1,259.158 Reynolds number, and water height reaches 0.86 m at the ship sides. It must be emphasised that this value is below the prop measure of 0.9 m. Strains are calculated at the minimum area which is defined by the size of each analysed element. The hull distributes generated strains along its axis. It should be pointed out this minimum value corresponds to 'superficial' resistance which because of the hull manufacture must have a material layer with minimum thickness. Since ANSYS FLUENT analyses the ship shape as geometry and not as solid, the increase of strain happens progressively at Y and Z axis; as the ship increases its speed, the strain reaches its maximum values of 0.97 Pa and 44.21 Pa, respectively.

It is demonstrated the place that takes the highest pressure is located at the hull tip. Its maximum static pressure is 1.91 MPa at seven knots of ship speed. Yet, dynamic pressure rises its value as water height increases, dynamic pressure reaches its maximum value of

7.32 MPa. As it can be seen during the collision of waves at the ship, water height level reaches the maximum value of 0.84 m.

Table 4 Results from the static analysis in relation to static, dynamic pressures, Reynolds number, turbulence intensity, water height reached during the simulation, different axis strains and convergence residuals

Ship speed	*Static pressure [Pa]*	*Dynamic pressure [Pa]*	*Reynolds number -*	*Turbulence intensity %*	*Water height [m]*	*Prow strains Y axis [Pa]*	*Prow strains Z axis [Pa]*	*Convergence residuals [Kg/s]*
4 knots–2,06 m/s	1,582.15	6,780.39	1′189.859	26.60	0.60	0.25	22.18	0.0081
6 knots–3,09 m/s	1,440.00	7,226.89	1′217.120.3	35.00	0.72	0.55	33.93	0.0000
7 knots–3,6 m/s	1,912.82	7,326.38	1′253.121.6	37.84	0.84	0.81	38.99	0.0001
8 knots–4,12 m/s	2,443.21	7,955.92	1′259.158	41.20	0.86	0.97	44.21	0.0002

Turbulence intensity is a dimensionless parameter, which depends on the analysis of fluid speed and calculated Reynolds number; therefore, it is expressed with percentages which indicate fluid speed at the proximity of the ship curves. The highest turbulence intensity was detected at the ship stern, which belongs to the simulation with current velocity at 3.6 m/s and 4.12 m/s for the ship. This explains that ship geometry has an arrow type of shape at the stern and prismatic geometry at prow. In Damjanović et al. (2010) can be seen that similar turbulence intensity values are obtained for the analysis case of an aerodynamic car, its average is 25% which shows that into water this parameter increases.

Dynamic simulation converges with a numeric value of 1E-4 in relation to presented convergence residuals. The ideal case would be 0% of error, yet this value is acceptable, since the total fluid analysis has less than 2% of error. Under INOCAR conditions and ship construction conditions, the simulation converged.

3.3 Validated results

Obtained results for validating the information in the static analysis are static pressure and water height gotten from the simulation and through mathematic calculation. This data is shown in Table 5. The results of ‘calculated’ and ‘simulated’ pressure match with a maximum error obtained, which is 5.77%. Reached water height and simulated ship speed were taken as reference to carry out calculations according to specified formulas at 2.6.1; therefore, these results are valid.

The results of dynamic pressure in the static case, calculated and simulated dynamic pressure and, simulated and calculated fluid velocity are shown at Table 6. As indicated in 2.6.2 the validation of the dynamic case, starts from pressure values and verifies whether velocity values through simulated and mathematical calculations are similar or not. It was obtained a maximum difference of 0.6 m/s; therefore, it can be taken as validated information.

Figure 4 Dynamic analysis results, (a) static pressure, (b) dynamic pressure, (c) Reynolds number, (d) fluid turbulence, (e) simulated water (see online version for colours)

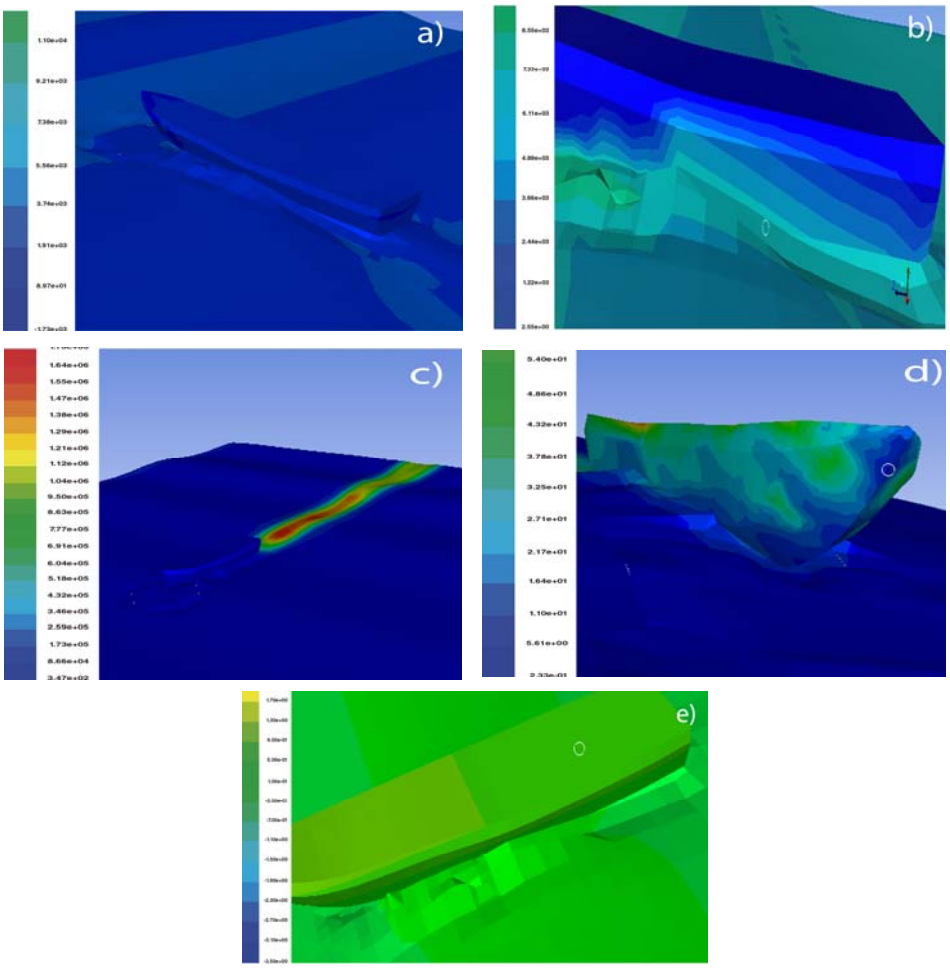

Table 5 Static pressure at static case validation of results for simulated fluid speed, simulated static pressure, calculated static pressure, simulated water height and calculated water height

Simulated fluid speed (m/s)	*Simulated static pressure (Pa)*	*Calculated static pressure (Pa)*	*Simulated water height (m)*	*Calculated water height (m)*
2.06	1,039.32	9,79.23	0.10	0.11
3.09	1,134.86	1,175.08	0.12	0.12
3.6	1,515.42	1,468.85	0.14	0.15
4.12	1,630.24	1,566.77	0.16	0.17

The same procedure was performed in order to analyse the obtained variation between 'simulated' and 'calculated' static pressure. It indicates that at speed of 3.08 m/s, the maximum error is 2% at 3.6 m/s. At 4.1 m/s the obtained maximum error is 0.02%. Obtained results are shown in Table 7.

Table 6 Dynamic pressure at static case

Calculated dynamic pressure (Pa)	*Simulated dynamic pressure (Pa)*	*Simulated fluid velocity (m/s)*	*Calculated fluid velocity (m/s)*
1,528.49	1,548.12	2.06	1.76
3,119.37	3,031.11	3.09	2.46
4,491.90	4,419.08	3.6	2.98
6,113.97	5,968.40	4.12	3.46

Note: Results of calculated/simulated dynamic pressure and simulated/calculated fluid velocity.

Table 7 Static pressure for dynamic case data validation

Simulated fluid velocity (m/s)	*Simulated static pressure (Pa)*	*Calculated static pressure (Pa)*	*Simulated water height (m)*	*Calculated water height (m)*
		–195.85	–0.02	–0.025
		979.23	0.1	0.12
3.08	1,440.00	1,468.85	0.15	0.17
3.6	1,912.82	1,958.47	0.2	0.26
4.1	2,443.21	2,448.09	0.25	0.38
		2,937.70	0.3	0.4

Likewise, the static case, validation starts from pressure values and verifies whether simulation and mathematic calculations of velocity values are similar or not. This values have a maximum difference is 0.7 m/s. 'Calculated' and 'simulated' values of dynamic pressure are close obtaining 3.48% of maximum error. Mathematical calculus implies theoretical validation of the obtained results considering initial conditions. The results were obtained across the keel of the ship, since maximum strains are produced along this axial axis; this element constitutes the cornerstone of the ship. The results are shown in Table 8.

Table 8 Dynamic pressure for dynamic case data validation

Calculated velocity (m/s)	*Calculated dynamic pressure (Pa)*	*Simulated fluid's velocity (m/s)*	*Simulated dynamic pressure (Pa)*
3.6	6,468.336		
3.7	6,832.679		6,780.38
3.8	7,207.004	3.09	7,226.89
3.9	7,591.311	3.6	7,326.38
4	7,985.60	4.12	7,955.92
4.1	8,389.871		

4 Conclusions

The present investigation achieved a simulation of a monohull ship under real operating conditions by ANSYS FLUENT. Verification of results has been done through theoretical formulas. Hence involves obtaining real values of a functional motorboat with

7.5 m length, which its results will lead to subsequent design. Static test conditions were selected where marine current hits the hull. Likewise, dynamic test conditions offshore were selected where the ship moves with velocity different from zero and reverse moving current. Correspondingly, theoretical formulas were used for validation.

Obtained results as static and dynamic pressures increase proportionally with marine current velocity. In addition, for both cases, applied water pressure is higher at the hull than the rest of the ship. Water collision with the hull produces the increase of water height. This produces splashes and low water volumes enter to the ship interior. However, the simulation shows that these volumes do not represent a risk for crew on board.

The present investigation supports hull bibliography studies of energy efficiency in ships including catamarans or trimarans. In this cases, the analysis can be separated for each one and lead to scientific work with the objective of classifying energy and efficiency parameters.

5 The future work

In order to reduce emissions of greenhouse gases from international shipping, the energy efficiency design index (EEDI) has been made compulsory for all new ships. Several steps in the form of new technologies and efficient design features have already been taken to ensure that the energy EEDI is met.

One of this is a synthesis of CAD and CFD is presently being attempted to achieve an efficient ship design, which might prove beneficial. Until some years ago when EEDI was not a prime concern, many ships were built in countries such as China due to heavy economic advantage of certain off-the-shelf standard design. But now, it is a welcome sign that that design after hydrodynamic analysis of hull form is being taken up for economic and academic betterment.

The present investigation supports hull bibliography studies of energy efficiency in ships including catamarans or trimarans for EEDI.

References

Acharya, S. and Biswal, M.P. (2016) 'Solving multi-choice multi-objective transportation problem', *International Journal of Mathematics in Operational Research*, Vol. 8, No. 4, pp.509–527.

Anderson, A. and Coughlan, B. (2006) 'Liquid film flows over solid surfaces', *6th MIRA International Vehicle Aerodynamics Conference*, pp.368–379.

ANSYS (2009) *Guide ANSYS Fluent-Solver Modeling*, Release 12.1.

ANSYS (2015) *Presión Hidrodinámica* [online] http://www.nysplm.com/ansys/calculo-fluidos-cfd.php (accessed 31 July 2018).

Azimi, K. and Solimanpur, M. (2016) 'A heuristic method to solve the location and machine selection problem in a two-dimensional continuous area', *International Journal of Mathematics in Operational Research*, Vol. 8, No. 4, pp.424–448.

Bartrons-Casademont, J. (2014) *Estudio hidrodinámico por CFD del casco de una lancha motora*, pp.31–65, Thesis degree, Politécnica University of Cataluña.

Beltran, D., Martínez-Gómez, J. and Lobato-Cordero, A. (2017) 'Effect of environment on the selection of phase change materials for building wallboards using multi-criteria decision methods and building energy simulations', *Proceedings of the 15th IBPSA Conference*, pp.1359–1369 [online] https://doi.org/10.26868/25222708.2017.349.

Chaloob, I.Z., Ramli, R. and Nawawi, M.K.M. (2016) 'A new multi-interval weights approach in fuzzy goal programming for a multi-criteria problem', *International Journal of Mathematics in Operational Research*, Vol. 9, No. 2, pp.214–229.

Damjanović, D., Kozak, D., Ivandić, Ž. and Kokanović, M. (2010) 'Car design as a new conceptual solution and CFD analysis in purpose of improving aerodynamics', *Josip Juraj Strossmayer*, University of Osijek, Croatia.

Dash, A.K., Nagarajan, V. and Sha, O.P. (2015) 'Bifurcation analysis of a high-speed twin-propeller twin-rudder ship maneuvering model in roll-coupling motion', *Nonlinear Dynamics*, Vol. 83, No. 4, pp.2035–2053.

De Leval, M.R., Dubini, G., Jalali, H. and Pietrabissa, R. (1996) 'Use of computational fluid dynamics in the design of surgical procedures: application to the study of competitive flows in cavopulmonary connections', *The Journal of Thoracic and Cardiovascular Surgery*, Vol. 111, No. 3, pp.502–513.

de Paz, C. (2011) *Presion Hidrostatica* [online] https://www.fullquimica.com/2011/04/presion-hidrostatica.html (accessed 31 July 2018).

Gaylard, A.P. and Duncan, B. (2011) 'Simulation of rear glass and body side vehicle soiling by road sprays', *SAE International Journal of Passenger Cars-Mechanical Systems*, Vol. 4, No. 1, pp.184–196.

Godoy-Vaca, L. et al. (2017) 'Analysis of solar chimneys in different climate zones-case of social housing in Ecuador', *IOP Conference Series: Materials Science and Engineering*, Vol. 245, No. 7, DOI: 10.1088/1757-899X/245/7/072045.

Hagemeier, T., Hartmann, M. and Thévenin, D. (2011) 'Practice of vehicle soiling investigations: a review', *International Journal of Multiphase Flow*, Vol. 37, No. 8, pp.860–875.

Heidarzade, A., Mahdavi, I. and Mahdavi-Amiri, N. (2016) 'Multiple attribute group decision making method using a new similarity measure in interval type-2 fuzzy sets: a case study', *International Journal of Mathematics in Operational Research*, Vol. 9, No. 2, pp.139–166.

Hirdaris, S.E., Bai, W., Dessi, D., Ergin, A., Gu, X., Hermundstad, O.A. and Fonseca, N. (2014) 'Loads for use in the design of ships and offshore structures', *Ocean Engineering*, Vol. 78, No. 1, pp.131–174.

INOCAR (2015) *Tabla de mareas* [online] https://www.inocar.mil.ec/web/index.php/tabla-demareas (accessed 31 July 2018).

Jongebloed, L. (2008) *Numerical Study using FLUENT of the Separation and Reattachment Points for Backwards-Facing Step Flow*, Doctoral dissertation, Rensselaer Polytechnic Institute.

Kastillo, J.P. et al. (2015) 'Computational fluid dynamic analysis of olive oil in different induction pots', *PANACM 2015 1st Pan-American Congress on Computational Mechanics*, Vol. 1, pp.729–742, DOI: 10.13140/RG.2.1.1487.6885.

Kastillo, J.P. et al. (2017) 'Thermal natural convection analysis of olive oil in different cookware materials for induction stoves', *International Journal of Food Engineering*, Vol. 13, No. 3, pp.1–15.

Kulczyk, T. and Górnicz, T. (2014) 'The analysis of motion dynamics and resistance of the multipurpose boat operating in shallow water', *TransNav: International Journal on Marine Navigation and Safety of Sea Transportation*, Vol. 8, No. 3, pp.359–363.

Martínez-Gómez, J. (2018) 'Material selection for multi-tubular fixed bed reactor Fischer-Tropsch reactor', *International Journal of Mathematics in Operational Research*, Vol. 13, No. 1, pp.1–29, DOI: 10.1504/IJMOR.2018.10013167.

Montiel, F., Bonnefoy, F., Ferrant, P., Bennetts, L.G., Squire, V.A. and Marsault, P. (2013) 'Hydroelastic response of floating elastic discs to regular waves, Part 1 wave basin experiments', *Journal of Fluid Mechanics*, Vol. 723, No. 1, pp.604–628.

Roettger, S., Schulz, M., Bartelheimer, W. and Ertlt, T. (2011) *Automotive Soiling Simulation Based on Massive Particle Tracing*, pp.309–317, Springer, Vienna.

Segura, C. and Remigio, J. (2016) *Modelación y simulación de un sistema híbrido de almacenamiento de energía eléctrica para la propulsión de embarcaciones tipo taxis en Puerto Ayora*, Master's thesis.

Shao, Y.L. and Faltinsen, O.M. (2012) 'A numerical study of the second-order wave excitation of ship springing in infinite water depth', *Proceedings of the Institution of Mechanical Engineers, Part M: Journal of Engineering for the Maritime Environment*, Vol. 226, No. 2, pp.103–119.

Singh, S., Zunaid, M., Ansari, N.A., Bahirani, S., Dhall, S. and Kumar, S. (2014) 'Numerical study of the generic sports utility vehicle design with a drag reduction add-on device', *Journal of Computational Engineering*, Vol. 2014, No. 1, pp.1–18, Article ID 785294.

Villacís, S. et al. (2015) 'Energy efficiency analysis of different materials for cookware commonly used in induction cookers', *Energy Procedia*, Vol. 75, pp.925–930, DOI: 10.1016/ j.egypro.2015.07.252.

Villacreses, G., Salinas, S.S., Ortiz, W.D., Villacís, S. and Martínez-Gómez, J. (2017) 'Environmental impact assessment of internal combustion and electric engines for maritime transport', *Environmental Processes*, Vol. 4, No. 4, pp.907–922.

Wu, Y.S. and Cui, W.C. (2009) 'Advances in the three-dimensional hydroelasticity of ships', *Proceedings of the Institution of Mechanical Engineers, Part M: Journal of Engineering for the Maritime Environment*, Vol. 223, No. 3, pp.331–348.

Yarrarapu, S.K., Mahaboob, M., Engineer, M. and Saitejkrushnarjuna, C. (2015) 'Significance of Skeg in course stability using computational fluid dynamics', *International Journal of Engineering Research and Technology*, Vol. 4, No. 7, pp.6–9, ESRSA Publications.